INSTITUTE OF PHYSICS PUBLISHING JOURNAL OF OPTICS B: QUANTUM AND SEMICLASSICAL OPTICS

J. Opt. B: Quantum Semiclass. Opt. **7** (2005) S616–S621 doi:10.1088/1464-4266/7/12/025

Squeezed Fock state by inconclusive photon subtraction

Stefano Olivares and Matteo G A Paris

Dipartimento di Fisica, Università degli Studi di Milano, Italy

E-mail: Stefano.Olivares@mi.infn.it and Matteo.Paris@fisica.unimi.it

Received 4 July 2005, accepted for publication 14 September 2005
Published 16 November 2005
Online at stacks.iop.org/JOptB/7/S616

Abstract

We analyse in detail the properties of the conditional state recently obtained by Wenger *et al* (2004 *Phys. Rev. Lett.* **92** 153601) by means of inconclusive photon subtraction (IPS) from a squeezed vacuum state $S(r)|0\rangle$. The IPS process can be characterized by two parameters: the IPS transmissivity τ and the photodetection quantum efficiency η. We found that the conditional state approaches the squeezed Fock state $S(r)|1\rangle$ when $\tau, \eta \to 1$, i.e., in the limit of single-photon subtraction. For nonunit IPS transmissivity and nonunit quantum efficiency, the conditional state remains close to the target state, i.e., shows a high fidelity, as long as the squeezing parameter is not too large. The purity and the nonclassicality of the conditional state are also investigated and a nonclassicality threshold on the IPS parameters is derived.

Keywords: non-Gaussian states, photon subtraction, conditional states

(Some figures in this article are in colour only in the electronic version)

1. Introduction

Beam splitters (BSs) and avalanche photodetectors (APDs) play a fundamental role in quantum information processing. These key elements, among the other applications, can be used together with conditional measurements in order to generate non-Gaussian states from Gaussian ones [1–4] and to distil continuous-variable entanglement [5].

In this paper we focus our attention on the output state recently obtained experimentally by Wenger *et al* [6] by means of photon subtraction from a squeezed vacuum state $S(r)|0\rangle$, $S(r)$ being the squeezing operator. More precisely, when a Gaussian state, such as $S(r)|0\rangle$, is mixed with the vacuum at a beam splitter and, then, on/off photodetection is performed on the reflected beam, an unknown number of photons is subtracted from the input state and the output state is no longer Gaussian, i.e., the input state is de-Gaussified: this is due to the fact that the positive operator valued measure (POVM) describing the APD is non-Gaussian. Since the actual number of detected photons cannot be resolved by the APD, in [3] we referred to this process as inconclusive photon subtraction (IPS). In general the IPS process can be characterized by two parameters: the beam splitter transmissivity τ and the quantum efficiency η of the APD. As we will see, the conditional output state obtained by IPS on a squeezed vacuum is close to the squeezed Fock state $S(r)|1\rangle$, which is otherwise difficult to produce by Hamiltonian processes. For this reason, we address IPS as an effective resource to generate these squeezed Fock states. We find that the IPS conditional state reduces to $S(r)|1\rangle$ in the limit $\tau, \eta \to 1$, whereas for different values of the transmissivity and of the quantum efficiency it remains close to this target state, showing a high fidelity for a wide range of the parameters. Finally, since the IPS state obtained from the squeezed vacuum is, in general, nonclassical and mixed, we study how the purity and the nonclassical depth of the IPS state depend on τ, η, and the input squeezing parameter r. Throughout the paper we will refer to $S(r)|1\rangle$ as to the target state of IPS on $S(r)|0\rangle$.

The paper is structured as follows: in section 2 we review the main elements of the IPS process on a single mode of radiation. The fidelity between the IPS conditional state and the squeezed Fock state $S(z)|1\rangle$, as well as its purity, is then investigated in section 3, whereas section 4 is devoted to the analysis of the nonclassicality of the IPS state. Finally, section 5 closes the paper with some concluding remarks.

2. The inconclusive photon subtraction process

The scheme of the inconclusive photon subtraction (IPS) process is sketched in figure 1. An input state $\varrho^{(\mathrm{in})}$ is mixed

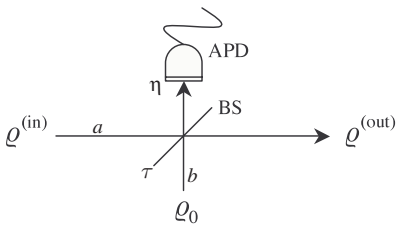

Figure 1. Scheme of the IPS process: the input state $\varrho^{(\mathrm{in})}$ is mixed with the vacuum state $\varrho_0 = |0\rangle\langle 0|$ at a beam splitter (BS) with transmissivity τ; then, avalanche photodetection (APD) with quantum efficiency η is performed on the reflected beam. When the detector clicks we obtain the IPS state $\varrho^{(\mathrm{out})}$.

with the vacuum state $\varrho_0 = |0\rangle\langle 0|$ at a beam splitter (BS) with transmissivity τ and, then, on/off avalanche photodetection (APD) with quantum efficiency η is performed on the reflected beam. Since the APD can only distinguish the presence from the absence of light, this measurement is *inconclusive*, namely it does not resolve the number of the detected photons. In this way, when the detector clicks, an unknown number of photons is *subtracted* from the initial state and we obtain the IPS state $\varrho^{(\mathrm{out})}$. Since the whole process is characterized by τ and η, we will also refer to them as IPS transmissivity and IPS quantum efficiency.

If the input state of the mode a is the squeezed vacuum state $\varrho_r^{(\mathrm{in})} = |0, r\rangle\langle 0, r|$, where $|0, r\rangle = S(r)|0\rangle$, $S(r) = \exp\{\frac{1}{2}r(a^{\dagger 2} - a^2)\}$ being the squeezing operator (for the sake of simplicity, without lack of generality, we can assume r as real), its (Gaussian) characteristic function $\chi_r^{(\mathrm{in})}(\boldsymbol{\Lambda}_a) \equiv \chi[\varrho_r^{(\mathrm{in})}](\boldsymbol{\Lambda}_a)$ reads

$$\chi_r^{(\mathrm{in})}(\boldsymbol{\Lambda}_a) = \exp\left\{-\tfrac{1}{2}\boldsymbol{\Lambda}_a^{\mathrm{T}}\boldsymbol{\sigma}_r\,\boldsymbol{\Lambda}_a\right\} \tag{1}$$

where $\boldsymbol{\Lambda} = (\mathrm{x}_a, \mathrm{y}_a)^{\mathrm{T}}$, $(\cdots)^{\mathrm{T}}$ being the transposition operation, and

$$\boldsymbol{\sigma}_r = \tfrac{1}{2}\begin{pmatrix} \mathrm{e}^{2r} & 0 \\ 0 & \mathrm{e}^{-2r} \end{pmatrix}, \tag{2}$$

is the covariance matrix. Analogously, the vacuum state $\varrho_0 = |0\rangle\langle 0|$ of the mode b is described by the (Gaussian) characteristic function

$$\chi_0(\boldsymbol{\Lambda}_b) \equiv \chi[\varrho_0](\boldsymbol{\Lambda}_b) = \exp\left\{-\tfrac{1}{2}\boldsymbol{\Lambda}_b^{\mathrm{T}}\boldsymbol{\sigma}_0\,\boldsymbol{\Lambda}_b\right\}, \tag{3}$$

where $\boldsymbol{\sigma}_0 = \frac{1}{2}\mathbb{I}_2$, $\mathbb{I}_2$ being the 2×2 identity matrix. Since the initial two-mode state $\varrho_r^{(\mathrm{in})} \otimes \varrho_0$ is Gaussian, under the action of the BS its 4×4 covariance matrix

$$\boldsymbol{\sigma}_{\mathrm{in}} = \left(\begin{array}{c|c} \boldsymbol{\sigma}_r & \boldsymbol{0} \\ \hline \boldsymbol{0} & \boldsymbol{\sigma}_0 \end{array}\right) \tag{4}$$

transforms as follows [7, 8]

$$\boldsymbol{\sigma}_{\mathrm{in}} \rightsquigarrow \boldsymbol{\sigma}' \equiv \boldsymbol{S}_{\mathrm{BS}}^{\mathrm{T}}\,\boldsymbol{\sigma}_{\mathrm{in}}\,\boldsymbol{S}_{\mathrm{BS}} \equiv \left(\begin{array}{c|c} \boldsymbol{A} & \boldsymbol{C} \\ \hline \boldsymbol{C}^{\mathrm{T}} & \boldsymbol{B} \end{array}\right), \tag{5}$$

where $\boldsymbol{A}$, $\boldsymbol{B}$, and $\boldsymbol{C}$ are 2×2 matrices and

$$\boldsymbol{S}_{\mathrm{BS}} = \left(\begin{array}{c|c} \sqrt{\tau}\,\mathbb{I}_2 & \sqrt{1-\tau}\,\mathbb{I}_2 \\ \hline -\sqrt{1-\tau}\,\mathbb{I}_2 & \sqrt{\tau}\;\mathbb{I}_2 \end{array}\right), \tag{6}$$

is the symplectic transformation associated with the evolution operator of the BS. Now, the on/off photodetector with quantum efficiency η can be described by the POVM $\{\Pi_{\mathrm{off}}(\eta), \Pi_{\mathrm{on}}(\eta)\}$, with

$$\Pi_{\mathrm{off}}(\eta) = \sum_{k=0}^{\infty}(1-\eta)^k|k\rangle\langle k|, \qquad \Pi_{\mathrm{on}}(\eta) = \mathbb{I} - \Pi_{\mathrm{off}}(\eta), \tag{7}$$

which corresponds to the characteristic functions

$$\chi[\Pi_{\mathrm{off}}(\eta)](\boldsymbol{\Lambda}) \equiv \chi_\eta^{(\mathrm{off})}(\boldsymbol{\Lambda}) = \frac{1}{\eta}\exp\left\{-\frac{1}{2}\boldsymbol{\Lambda}^{\mathrm{T}}\boldsymbol{\sigma}_{\mathrm{M}}\,\boldsymbol{\Lambda}\right\}, \tag{8}$$

$$\chi[\Pi_{\mathrm{on}}(\eta)](\boldsymbol{\Lambda}) \equiv \chi_\eta^{(\mathrm{on})}(\boldsymbol{\Lambda}) = 2\pi\delta^{(2)}(\boldsymbol{\Lambda}) - \chi_\eta^{(\mathrm{off})}(\boldsymbol{\Lambda}), \tag{9}$$

respectively, $\delta^{(2)}(\boldsymbol{\Lambda})$ being the two-dimensional Dirac delta function, and

$$\boldsymbol{\sigma}_{\mathrm{M}} = \frac{2-\eta}{2\eta}\,\mathbb{I}_2. \tag{10}$$

The probability of a click in the detector is then given by [8, 9]

$$p_{\mathrm{on}}(r,\tau,\eta) = \mathrm{Tr}_{ab}[\varrho'_{r,\tau}\,\mathbb{I}\otimes\Pi_{\mathrm{on}}(\eta)] \tag{11}$$

$$= \frac{1}{(2\pi)^2}\int_{\mathbb{R}^4}\mathrm{d}^2\boldsymbol{\Lambda}_a\,\mathrm{d}^2\boldsymbol{\Lambda}_b\,\chi[\varrho'_{r,\tau}](\boldsymbol{\Lambda}_a,\boldsymbol{\Lambda}_b) \times \chi[\mathbb{I}](-\boldsymbol{\Lambda}_a)\,\chi_\eta^{(\mathrm{on})}(-\boldsymbol{\Lambda}_b) \tag{12}$$

$$= 1 - \left(\eta\sqrt{\mathrm{Det}[\boldsymbol{B}+\boldsymbol{\sigma}_{\mathrm{M}}]}\right)^{-1}$$

$$= 1 - \left(\sqrt{1+(1-\tau_{\mathrm{eff}}^2)\sinh^2 r}\right)^{-1}, \tag{13}$$

where $\chi[\varrho'_{r,\tau}](\boldsymbol{\Lambda}_a,\boldsymbol{\Lambda}_b)$ is the two-mode characteristic function associated with the state $\varrho'_{r,\tau} \equiv U_{\mathrm{BS}}\,\varrho_r^{(\mathrm{in})}\otimes\varrho_0\,U_{\mathrm{BS}}^\dagger$, $\chi[\mathbb{I}](\boldsymbol{\Lambda}) = 2\pi\delta^{(2)}(\boldsymbol{\Lambda})$, and $\tau_{\mathrm{eff}} \equiv \tau_{\mathrm{eff}}(\tau,\eta) = 1-\eta(1-\tau)$. Note that when $\tau_{\mathrm{eff}} \to 1$, the probability (13) can be approximated at the first order in τ_{eff} as follows:

$$p_{\mathrm{on}}(r,\tau,\eta) = (1-\tau_{\mathrm{eff}})\sinh^2 r + \mathrm{o}\left[(1-\tau_{\mathrm{eff}})^2\right]. \tag{14}$$

Finally, the output state

$$\varrho_{r,\tau,\eta}^{(\mathrm{out})} = \frac{\mathrm{Tr}_b[\varrho'_{r,\tau}\,\mathbb{I}\otimes\Pi_{\mathrm{on}}(\eta)]}{p_{\mathrm{on}}(r,\tau,\eta)}, \tag{15}$$

conditioned to a click of the on/off photodetector, has the characteristic function $\chi_{r,\tau,\eta}^{(\mathrm{out})}(\boldsymbol{\Lambda}_a) \equiv \chi[\varrho_{r,\tau,\eta}^{(\mathrm{out})}](\boldsymbol{\Lambda}_a)$ [9]:

$$\chi_{r,\tau,\eta}^{(\mathrm{out})}(\boldsymbol{\Lambda}_a) = \frac{1}{2\pi\;p_{\mathrm{on}}(r,\tau,\eta)} \times \int_{\mathbb{R}^2}\mathrm{d}^2\boldsymbol{\Lambda}_b\,\chi[\varrho'_{r,\tau}](\boldsymbol{\Lambda}_a,\boldsymbol{\Lambda}_b)\,\chi_\eta^{(\mathrm{on})}(-\boldsymbol{\Lambda}_b) \tag{16}$$

$$= \frac{1}{p_{\mathrm{on}}(r,\tau,\eta)}\left\{\exp\left\{-\frac{1}{2}\boldsymbol{\Lambda}_a^{\mathrm{T}}\,\boldsymbol{\Sigma}_1\,\boldsymbol{\Lambda}_a\right\} - \frac{\exp\left\{-\frac{1}{2}\boldsymbol{\Lambda}_a^{\mathrm{T}}\,\boldsymbol{\Sigma}_2\,\boldsymbol{\Lambda}_a\right\}}{\eta\sqrt{\mathrm{Det}[\boldsymbol{B}+\boldsymbol{\sigma}_{\mathrm{M}}]}}\right\}, \tag{17}$$

with $\boldsymbol{\Sigma}_1 = \boldsymbol{A}$ and $\boldsymbol{\Sigma}_2 = \boldsymbol{A} - \boldsymbol{C}(\boldsymbol{B}+\boldsymbol{\sigma}_{\mathrm{M}})^{-1}\boldsymbol{C}^{\mathrm{T}}$. Note that the output state is no longer a Gaussian state, namely its characteristic function is no longer Gaussian: for this reason the IPS process is also referred to as a *de-Gaussification* process [6].

In general, a Gaussian state described by the characteristic function (in Cartesian notation, namely $\mathbf{\Lambda} = (\mathsf{x}, \mathsf{y})^{\mathrm{T}}$)

$$\chi(\mathbf{\Lambda}) = \exp\left\{-\tfrac{1}{2}\mathbf{\Lambda}^{\mathrm{T}}\boldsymbol{\sigma}\,\mathbf{\Lambda}\right\} \tag{18}$$

with covariance matrix

$$\boldsymbol{\sigma} = \begin{pmatrix} \mathsf{a} & \mathsf{c} \\ \mathsf{c} & \mathsf{b} \end{pmatrix}, \tag{19}$$

can be also written in the complex notation as follows:

$$\chi(\lambda) = \exp\left\{-\mathcal{A}|\lambda|^2 - \mathcal{B}\lambda^2 - \mathcal{B}^*\lambda^{*2}\right\}, \tag{20}$$

with

$$\mathcal{A} = \tfrac{1}{2}(\mathsf{a}+\mathsf{b}), \qquad \mathcal{B} = \tfrac{1}{4}(\mathsf{b}-\mathsf{a}+2\mathsf{i}\mathsf{c}), \tag{21}$$

where we introduced the complex number $\lambda = \frac{1}{\sqrt{2}}(\mathsf{x}+\mathsf{i}\mathsf{y})$. In this way, the characteristic function (17) can be written as follows:

$$\chi^{(\mathrm{out})}_{r,\tau,\eta}(\lambda) = \frac{\exp\left\{-\mathcal{A}_1|\lambda|^2 - \mathcal{B}_1\lambda^2 - \mathcal{B}_1^*\lambda^{*2}\right\}}{p_{\mathrm{on}}(r,\tau,\eta)} - \frac{\exp\left\{-\mathcal{A}_2|\lambda|^2 - \mathcal{B}_2\lambda^2 - \mathcal{B}_2^*\lambda^{*2}\right\}}{p_{\mathrm{on}}(r,\tau,\eta)\,\eta\sqrt{\mathrm{Det}[\boldsymbol{B}+\boldsymbol{\sigma}_{\mathrm{M}}]}}, \tag{22}$$

where $\mathcal{A}_k$ and $\mathcal{B}_k$ refer to the covariance matrix $\mathbf{\Sigma}_k$, $k = 1, 2$ respectively. Finally, using the definition

$$W[\varrho](\alpha) = \frac{1}{\pi^2}\int_{\mathbb{C}} \mathrm{d}^2\lambda\, \chi[\varrho](\lambda)\, \exp\left\{\lambda^*\alpha - \alpha^*\lambda\right\}, \tag{23}$$

which relates the Wigner function $W[\varrho](\alpha)$ of a state ϱ to its characteristic function $\chi[\varrho](\lambda)$, one can obtain the Wigner function $W^{(\mathrm{out})}_{r,\tau,\eta}(\alpha) \equiv W[\varrho^{(\mathrm{out})}_{r,\tau,\eta}](\alpha)$. As for the characteristic function, to pass from the complex, $W[\varrho](\alpha)$, to the Cartesian notation, $W[\varrho](x, y)$, one should put $\alpha = \frac{1}{\sqrt{2}}(x + \mathrm{i}y)$ [8]. In figure 2(*a*) we report $W^{(\mathrm{out})}_{r,\tau,\eta}(x, y)$ for fixed r, τ, and η: as apparent from the plot the Wigner function is not Gaussian, and may assume negative values [6]. In section 4 we will investigate this effect by analysing the nonclassicality of the conditioned state. In figure 2(*b*) we show the Wigner function $\chi^{(\mathrm{SqF})}_z(x, y)$ associated with the squeezed Fock state $\varrho^{(\mathrm{SqF})}_z = S(z)|1\rangle\langle 1|S^\dagger(z)$, whose characteristic function $\chi^{(\mathrm{SqF})}_z(\lambda) \equiv \chi[\varrho^{(\mathrm{SqF})}_z](\lambda)$ reads (we assume z as real)

$$\chi^{(\mathrm{SqF})}_z(\lambda) = \left[1 - 2\left(\mathcal{A}_0|\lambda|^2 + \mathcal{B}_0\lambda^2 + \mathcal{B}_0^*\lambda^{*2}\right)\right] \times \exp\left\{-\mathcal{A}_0|\lambda|^2 - \mathcal{B}_0\lambda^2 - \mathcal{B}_0^*\lambda^{*2}\right\}, \tag{24}$$

with $\mathcal{A}_0 = 2(\cosh^2 z + \sinh^2 z)$ and $\mathcal{B}_0 = -2\cosh z\,\sinh z$. Since the Wigner functions of the IPS squeezed vacuum and of the squeezed number state are quite similar, one can think of using the IPS process to produce the state $\varrho^{(\mathrm{SqF})}_r$; motivated by this consideration, in the next section we will analyse the fidelity between these states. Figure 3 shows $W^{(\mathrm{out})}_{r,\tau,\eta}(x, y)$ with fixed r and η and different values of the IPS transmissivity τ; the plots on the right of the same figure compare the $W^{(\mathrm{out})}_{r,\tau\eta}(0, y)$ (solid lines) with $W^{(\mathrm{SqF})}_r(0, y)$ (dashed line). Finally, the effect of the quantum efficiency η on the output state is shown in figure 4, where we plot as reference the value of the Wigner function $W^{(\mathrm{out})}_{r,\tau,\eta}$ at the centre of the complex plane as a function of the transmissivity τ and different values of η: we can see that the main effect on the output state is due to τ.

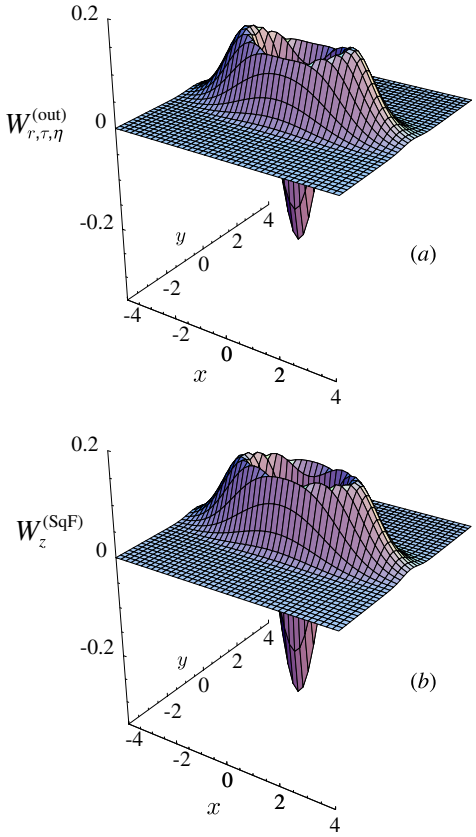

Figure 2. (*a*) Plot of the Wigner function $W^{(\mathrm{out})}_{r,\tau,\eta}(x, y)$ with $r = 0.5$, $\tau = 0.90$, and $\eta = 0.80$; (*b*) plot of the Wigner function $W^{(\mathrm{SqF})}_z(x, y)$ of the state $S(z)|1\rangle$ with squeezing parameter $z = 0.5$.

3. Fidelity and purity

The fidelity between the pure state $\varrho^{(\mathrm{SqF})}_z$ and the IPS state $\varrho^{(\mathrm{out})}_{r,\tau,\eta}$ is defined as follows:

$$F_{\tau,\eta}(z, r) = \mathrm{Tr}[\varrho^{(\mathrm{SqF})}_z\,\varrho^{(\mathrm{out})}_{r,\tau,\eta}] \tag{25}$$

$$= \frac{1}{2\pi}\int_{\mathbb{R}^2} \mathrm{d}^2\mathbf{\Lambda}\, \chi^{(\mathrm{SqF})}_z(\mathbf{\Lambda})\, \chi^{(\mathrm{out})}_{r,\tau,\eta}(-\mathbf{\Lambda}), \tag{26}$$

$$= \frac{1}{p_{\mathrm{on}}(r,\tau,\eta)}\left\{\mathcal{F}_1 - \frac{\mathcal{F}_2}{\eta\sqrt{\mathrm{Det}[\boldsymbol{B}+\boldsymbol{\sigma}_{\mathrm{M}}]}}\right\}, \tag{27}$$

where

$$\mathcal{F}_k = \frac{\mathcal{A}_k^2 - \mathcal{A}_0^2 - 4(\mathcal{B}_k^2 - \mathcal{B}_0^2)}{[(\mathcal{A}_0+\mathcal{A}_k)^2 - 4(\mathcal{B}_0+\mathcal{B}_k)^2]^{3/2}} \tag{28}$$

and $\mathcal{A}_h$ and $\mathcal{B}_h$, $h = 0, 1, 2$, have been introduced in equations (24) and (22), respectively. The analytic expression of $F_{\tau,\eta}(z, r)$ is quite cumbersome, but, on the other hand, we can draw some interesting considerations by addressing its expansion at the first order in the transmissivity τ when $\tau \to 1$ and $\eta = 1$, namely

$$F_{\tau,1}(z, r) = \frac{1}{\cosh^3(r-z)} - \left[\frac{9\cosh(r+z) - 3\cosh(3r-z)}{8\cosh(r-z)} - \frac{1}{4}\right](1-\tau) + \mathrm{o}\left[(1-\tau)^2\right]. \tag{29}$$

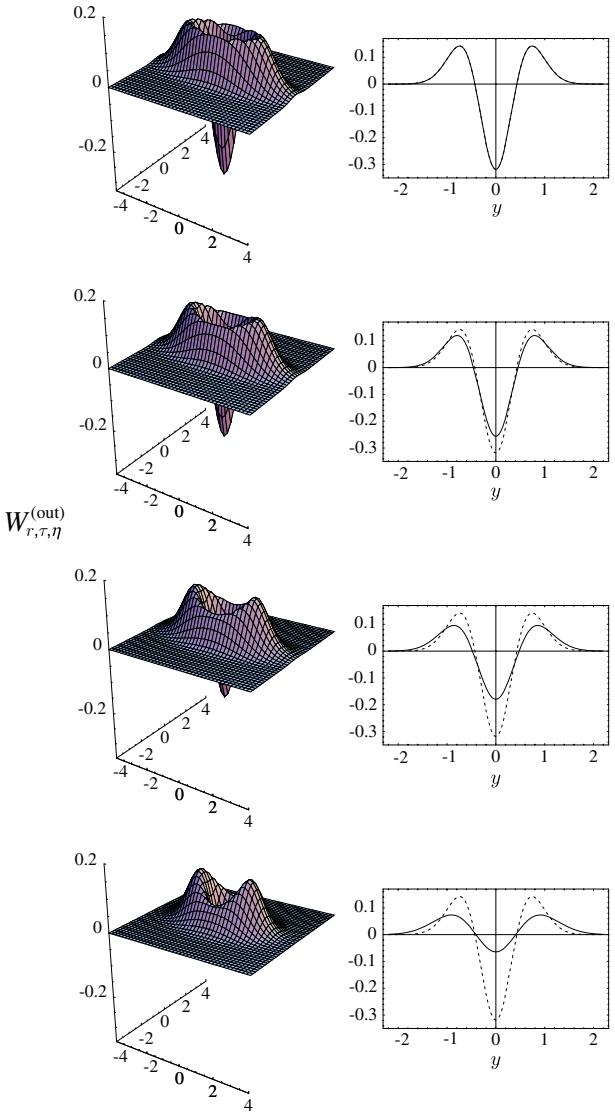

Figure 3. Plots of the Wigner function $W^{(\mathrm{out})}_{r,\tau,\eta}(x, y)$ with $r = 0.5$, $\eta = 0.80$, and different values of the BS transmissivity τ: from top to bottom $\tau = 0.99$, 0.9, 0.75, and 0.50. The solid lines of the plots on the right refer to $W^{(\mathrm{out})}_{r,\tau\eta}(0, y)$ whereas the dashed lines are $W^{(\mathrm{SqF})}_{z}(0, y)$ of the state $S(z)|1\rangle$ with squeezing parameter $z = 0.5$. Note that when $\tau = 0.99$ the two lines overlap. y is the squeezed coordinate.

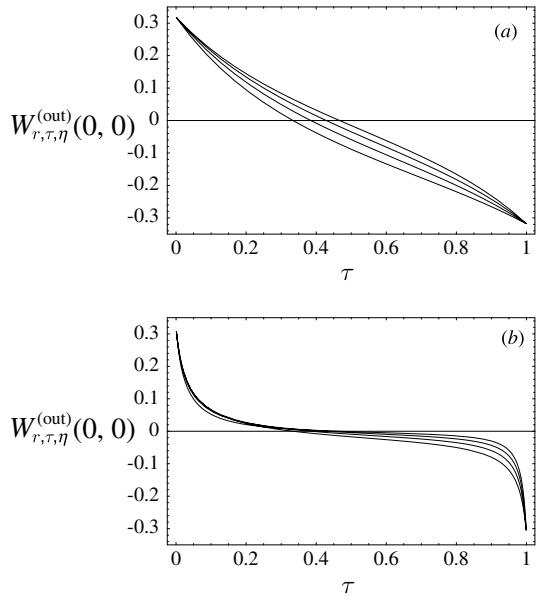

Figure 4. Plots of $W^{(\mathrm{out})}_{r,\tau,\eta}(0, 0)$ with (*a*) $r = 0.5$ and (*b*) $r = 2.0$ as a function of τ and different values of η: from bottom to top $\eta = 1.0$, 0.75, 0.50, and 0.25. The value of the function is mainly affected by τ.

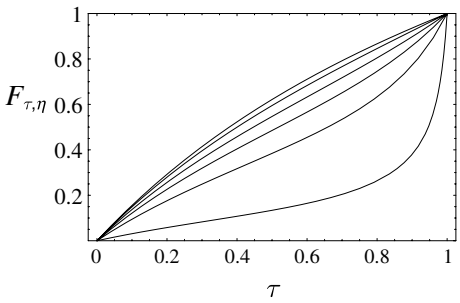

Figure 5. Plot of the fidelity $F_{\tau,\eta}(r)$ with $\eta = 0.80$ as a function of the IPS transmissivity τ for different values of r: from top to bottom $r = 0.1$, 0.3, 0.5, 0.7, 1.0, and 2.0.

In fact, from the expansion (29) we conclude that the maximum of the fidelity is achieved when $z = r$.

In figure 5 we plot $F_{\tau,\eta}(r) \equiv F_{\tau,\eta}(r, r)$ as a function of the IPS transmissivity and for different values of r. We can see that $F_{\tau,\eta}$ reaches its maximum when the IPS transmissivity approaches unity, namely in the single-photon subtraction limit [3]. Moreover, when the squeezing parameter r increases the fidelity decreases: this is due to the increasing (unknown) number of subtracted photons, which reduces the *purity* of the IPS state itself. In figure 6 we plot the purity $\mu_{\tau,\eta}(r)$ of the IPS squeezed vacuum $\varrho^{(\mathrm{out})}_{r,\tau,\eta}$, defined as follows [10]:

$$\mu_{\tau,\eta}(r) = \mathrm{Tr}\left[(\varrho^{(\mathrm{out})}_{r,\tau,\eta})^2\right] = \pi \int_{\mathbb{C}} \mathrm{d}^2\alpha \left[W^{(\mathrm{out})}_{r,\tau,\eta}(\alpha)\right]^2 \tag{30}$$

$$= \frac{1}{2p_{\mathrm{on}}(r, \tau, \eta)} \left\{ \frac{1}{\sqrt{\mathcal{A}_1^2 - 4\mathcal{B}_1^2}} + \frac{1}{\eta^2\,\mathrm{Det}[\boldsymbol{B} + \boldsymbol{\sigma}_{\mathrm{M}}]\sqrt{\mathcal{A}_1^2 - 4\mathcal{B}_1^2}} - \frac{4}{\eta\sqrt{\mathrm{Det}[\boldsymbol{B} + \boldsymbol{\sigma}_{\mathrm{M}}]}\sqrt{(\mathcal{A}_1 + \mathcal{A}_2)^2 - 4(\mathcal{B}_1 + \mathcal{B}_2)^2}} \right\}. \tag{31}$$

4. Nonclassicality of the IPS squeezed vacuum state

As a measure of nonclassicality of the IPS state $\varrho^{(\mathrm{out})}_{r,\tau,\eta}$ we consider the *nonclassical depth* [11]

$$\mathcal{T} = \frac{1 - \overline{s}}{2}, \tag{32}$$

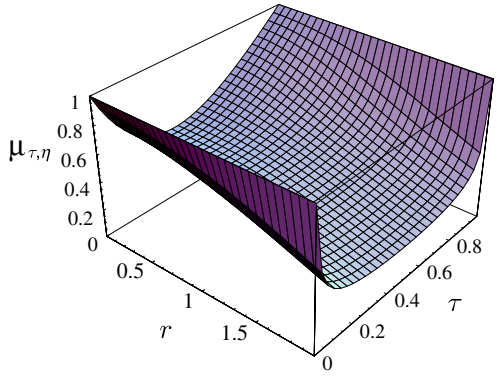

Figure 6. Plot of the purity $\mu_{\tau,\eta}(r)$ of the state $\varrho^{(\mathrm{out})}_{r,\tau,\eta}$. We set $\eta = 0.80$.

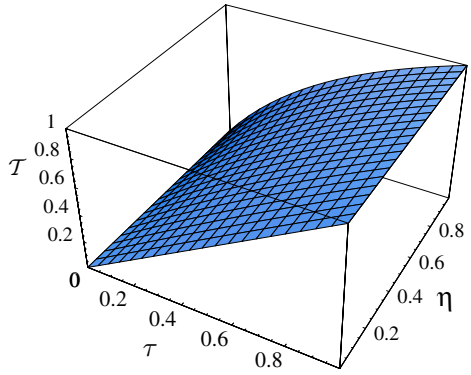

Figure 7. Plot of the nonclassical depth $\mathcal{T}(\tau, \eta)$ of the IPS squeezed vacuum state.

$\overline{s}$ being the maximum s for which the generalized quasi-probability function

$$W_s(\alpha) = \frac{1}{\pi}\int_{\mathbb{C}} \mathrm{d}^2\lambda\, \chi(\lambda)\, \exp\left\{\frac{1}{2}s + \lambda^*\alpha - \alpha^*\lambda\right\} \tag{33}$$

is a probability distribution, i.e. positive semidefinite and nonsingular. As a matter of fact, one has $\mathcal{T} = 1$ for number states and $\mathcal{T} = 0$ for coherent states. Moreover, the nonclassical depth can be interpreted as the minimum number of thermal photons which has to be added to a quantum state in order to erase all the quantum features of the state [8, 11]. In the case of $\varrho^{(\mathrm{out})}_{r,\tau,\eta}$, we have (for the sake of simplicity we do not write explicitly the dependence on r,τ and η in the symbol $W^{(\mathrm{out})}_s(\alpha)$)

$$W^{(\mathrm{out})}_s(\alpha) = \frac{1}{p_{\mathrm{on}}(r,\tau,\eta)}\left\{\mathcal{G}_1(\alpha) - \frac{\mathcal{G}_2(\alpha)}{\eta\sqrt{\mathrm{Det}[\boldsymbol{B}+\boldsymbol{\sigma}_{\mathrm{M}}]}}\right\} \tag{34}$$

where we defined

$$\mathcal{G}_k(\alpha) = \frac{2\,\exp\left\{-\dfrac{2(2\mathcal{A}_k - s)|\alpha|^2 + 4\mathcal{B}_k^*\alpha^2 + 4\mathcal{B}_k\alpha^{*2}}{(2\mathcal{A}_k - s)^2 - 16|\mathcal{B}_k|^2}\right\}}{\pi\sqrt{(2\mathcal{A}_k - s)^2 - 16|\mathcal{B}_k|^2}}. \tag{35}$$

At first we note that in order to have $W^{(\mathrm{out})}_s(\alpha)$ normalizable the following condition should be satisfied:

$$s \leqslant 2\mathcal{A}_k \qquad (k = 1, 2). \tag{36}$$

Furthermore, since $W^{(\mathrm{out})}_s(\alpha)$ is a difference between two Gaussian functions with the centre in the origin of the complex plane, one can easily see that, in general, this function has a minimum in $\alpha = 0$ and that this minimum can be negative. For this reason and thanks to other simple considerations about the symmetries of $W^{(\mathrm{out})}_s(\alpha)$ with respect to the point $\alpha = 0$, we can focus our attention on the origin of the complex plane, obtaining this further condition for the positivity:

$$\mathcal{G}_1(0) - \frac{\mathcal{G}_2(0)}{\eta\sqrt{\mathrm{Det}[\boldsymbol{B}+\boldsymbol{\sigma}_{\mathrm{M}}]}} \geqslant 0, \tag{37}$$

which, together with the conditions (36), brings us to

$$\overline{s}(\tau,\eta) = \frac{2 - \eta - (4-\eta)\tau}{2 - (1-\tau)\eta}, \tag{38}$$

and, then, to the following expression for the nonclassical depth:

$$\mathcal{T}(\tau,\eta) = \frac{2\tau}{2 - (1-\tau)\eta}. \tag{39}$$

Since $\mathcal{T}(\tau,\eta) \geqslant 0$, the conditional state is nonclassical for any nonzero value of the IPS transmissivity and efficiency. Note that equation (39) depends only on τ and η, whereas it is independent of the squeezing parameter r. Notice, however, that the nonclassical depth does not measure the extension of the negativity region, but only the presence of negative values. Therefore it is not surprising that equation (39) does not depend on r. We plot $\mathcal{T}(\tau,\eta)$ in figure 7. Since the usual Wigner function is obtained when $s = 0$ in (33), from equation (38) we can see that $W^{(\mathrm{out})}_{r,\tau,\eta}(\alpha)$ becomes positive semi-definite when $\tau = (2-\eta)/(4-\eta)$.

5. Concluding remarks

We have analysed in detail the state obtained by subtracting photons from the squeezed vacuum by means of linear optics, namely using beam splitters and avalanche photodetectors. We referred to the whole photon-subtraction process as inconclusive photon subtraction (IPS), since avalanche photodetectors are not able to resolve the number of detected photons. We found that the IPS conditional state obtained from a squeezed vacuum state is close to the squeezed Fock state $S(r)|1\rangle$ and approaches this target state when only one photon is subtracted, namely, using a high-transmissivity beam splitter for the IPS. Moreover, when the transmissivity and the quantum efficiency are not unity, the output state remains close to the target state, showing a high fidelity as long as the squeezing parameter is not too large. The purity and the nonclassicality of the IPS squeezed vacuum state have also been considered: we found that the relevant parameter is the transmissivity τ, while the IPS efficiency η only slightly affects the output state. We conclude that IPS, which was recently experimentally implemented [6], can be effectively used to produce a nonclassical state such as the squeezed Fock state $S(r)|1\rangle$, whose generation would otherwise be quite challenging.

References

[1] Opatrný T, Kurizki G and Welsch D-G 2000 *Phys. Rev.* A **61** 032302

[2] Cochrane P T, Ralph T C and Milburn G J 2002 *Phys. Rev.* A **65** 062306

[3] Paris M G A 2001 *Phys. Lett.* A **289** 167
Olivares S, Paris M G A and Bonifacio R 2003 *Phys. Rev.* A **67** 032314

[4] Olivares S and Paris M G A 2004 *Phys. Rev.* A **70** 032112

[5] Eisert J, Browne D E, Scheel S and Plenio M B 2004 *Ann. Phys.* **311** 431
Browne D E, Eisert J, Scheel S and Plenio M B 2003 *Phys. Rev.* A **67** 062320

[6] Wenger J, Tualle-Bouri R and Grangier P 2004 *Phys. Rev. Lett.* **92** 153601

[7] Arvind, Dutta B, Mukunda N and Simon R 1995 *J. Phys.* **45** 471 (*Preprint* quant-ph/9509002)

[8] Ferraro A, Olivares S and Paris M G A 2005 *Gaussian States in Quantum Information* (Napoli: Bibliopolis) (*Preprint* quant-ph/0503237)

[9] Eisert J, Scheel S and Plenio M B 2002 *Phys. Rev. Lett.* **89** 137903

[10] Paris M G A, Illuminati F, Serafini A and De Siena S 2003 *Phys. Rev.* A **68** 012314
Kim M S, Lee J and Munro W J 2002 *Phys. Rev.* A **66** 030301

[11] Lee C T 1991 *Phys. Rev.* A **44** R2775